Band-to-Band Misregistration of the Images of MODIS On-Board Calibrators and Its Impact to Calibration

Zhipeng Wang, *Member IEEE*, and Xiaoxiong Xiong

Abstract—The MODIS instruments aboard Terra and Aqua satellites are radiometrically calibrated on-orbit with a set of on-board calibrators (OBC) including a solar diffuser (SD), a blackbody (BB) and a space view (SV) port through which the detectors can view the dark space. As a whisk-broom scanning spectroradiometer, thirty-six MODIS spectral bands are assembled in the along-scan direction on four focal plane assemblies (FPA). These bands capture images of the same target sequentially with the motion of a scan mirror. Then the images are co-registered on board by delaying appropriate band-dependent amount of time depending on the band locations on the FPA. While this co-registration mechanism is functioning well for the "far field" remote targets such as Earth view (EV) scenes or the Moon, noticeable band-to-band misregistration in the along-scan direction has been observed for "near field" targets, in particular the OBCs. In this paper, the misregistration phenomenon is presented and analyzed. It is concluded that the root cause of the misregistration is that the rotating element of the instrument, the scan mirror, is displaced from the focus of the telescope primary mirror. The amount of the misregistration is proportional to the band location on the FPA and is inversely proportional to the distance between the target and the scan mirror. The impact of this misregistration to the calibration of MODIS bands is discussed. In particular, the calculation of the detector gain coefficient m_1 of bands 8-16 (412 nm – 870 nm) is improved by up to 1.5% for Aqua MODIS.

Index Terms— MODIS, calibration, optical design, image registration

I. INTRODUCTION

THE Moderate resolution imaging spectroradiometer (MODIS) is a key instrument aboard NASA's Terra and Aqua satellites that provides measurements of large-scale global dynamics in the oceans, on the land, and in the lower atmosphere [1], [2]. MODIS captures spectral images of high radiometric sensitivity in 20 reflective solar bands (RSB) (B1-B19 and B26) and 16 thermal emissive bands (TEB) (B20-B25, B27-B36), covering a spectral range from 0.4 to 14.4 µm. It is a passive whisk-broom scanning spectro-radiometer, with a rotating mirror scanning across its moving track. At a

Z. Wang is with Science Systems and Applications Inc., Greenbelt,, MD 20706, USA (phone: 301-867-2086; fax: 301-552-5223; e-mail: zhipeng.wang@ssaihq.com).
X. Xiong is with NASA Goddard Space Flight Center, Greenbelt, MD 20771, USA (email: Xiaoxiong.Xiong-1@nasa.gov).

nominal altitude of 705 km, the double-sided scan mirror rotates at a rate of 20.31 rpm and captures a swath of Earth view (EV) scene of 2330 km in the along-scan direction and 10 km at nadir in the along-track direction within an instrument scan. MODIS bands are located on four separate focal plane assemblies (FPA): visible (VIS), near-infrared (NIR), short-wave and mid-wave infrared (SMIR), and long-wave infrared (LWIR). Within a FPA, different bands are laid out in the along-scan direction and the detectors within a band are laid out in the along-track direction. The ground spatial resolutions at nadir for bands 1-2, bands 5-7 and bands 8-36 are 250 m, 500 m and 1 km, respectively.

The MODIS images of all bands are radiometrically calibrated. The instrument has a set of unprecedented on-board calibrators (OBCs), including a blackbody (BB), a solar diffuser (SD), a solar diffuser stability monitor (SDSM), and the spectroradiometric calibration assembly (SRCA), to provide radiometric, spectral, and spatial calibration. It also has a space view (SV) port through which the detectors can view the deep space for background signals and occasionally the Moon. The BB is the primary calibration source for TEB at 3.5-14.4 µm. The reflected solar illumination from the SD is the calibration source for RSB at 0.4-2.2 µm, with the SDSM tracking the degradation in the reflectance of the SD. The SRCA is a complex, multi-function calibration component that provides in-flight spectral, radiometric, and spatial calibration. Figure 1 is a sketch of the layout of these OBCs within MODIS cavity.

Within a MODIS scan, the scan mirror alternately directs light from SD, SRCA, BB, SV and EV scenes to MODIS detectors, as is shown in Fig. 2. The data are sampled at 3-kHz frequency so each data frame in the along-scan direction is acquired every 333.333 µs. The shades in Fig.2 represent the periods of time when the images are captured. The EV sector continuously captures 1354 frames of EV images, corresponding to a mirror scan angle range of -55 to 55 degrees. The cavity, however, is not continuously sampled. Fifty frames of images are acquired for SD, BB and SV each and 10 frames of images are acquired for SRCA. The sampled regions are narrower than the width of the OBCs, ensuring it is the center portion of the OBCs, where the surface property is more stable, that are sampled.

Images of various MODIS bands are spatially co-registered in the along-scan direction on board to view the same target
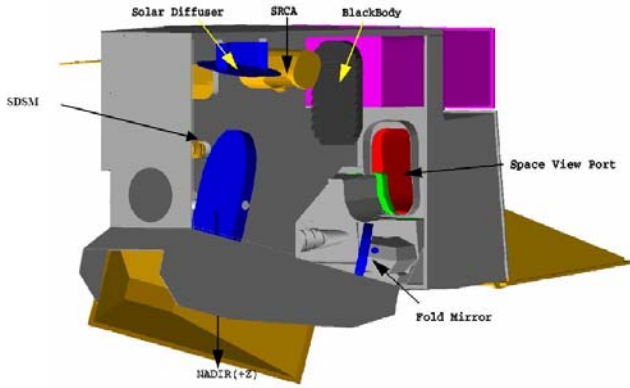
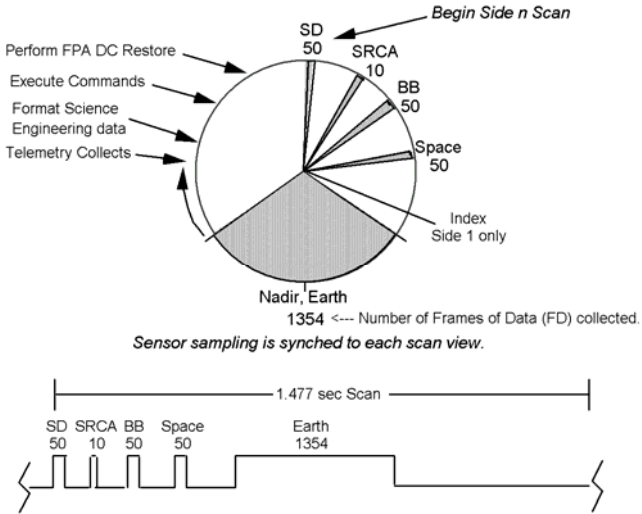Fig. 1. A diagram of MODIS cavity with its OBCs.

Fig. 2. The viewing sequence within a MODIS scan. Image are captured in units of frame during the shaded areas of the scan sequence (top) or the pulses (bottom).

within the same frame range. In this study, we show that the images of the OBCs are not perfectly co-registered. The amount of misregistration is related to the band location on the FPA and becomes more significant when the targets approach the scan mirror. This paper presents the results of investigating the phenomenon and analyzing its impact to MODIS calibration. In Section II, an overview of the band locations on the FPA and the on-board image co-registration process is provided. Section III introduces the observed image misregistration for the OBCs and illustrates how it is related to the band location on the FPA. The root cause of the misregistration is provided. The impact of the misregistration to MODIS calibration for both RSB and TEB is discussed in Section IV. Concluding remarks and a summary of this paper are given in Section V.

II. BAND LOCATION ON FPA AND IMAGE CO-REGISTRATION

The layout of MODIS bands on the FPAs is shown in Fig. 3 with scale [3]. The band locations on the FPA can be quantified in units of data frame or color period (333.333 μs) as a result of instrument design. The scan mirror sequentially directs the light from the same EV scene to various bands with B30 as the leading band and B32 as the trailing band. Therefore, the same target is actually sampled in different

TABLE I
NOMINAL BAND LOCATION ON THE MODIS FPA WITH RESPECT TO THE OPTICAL AXIS (IN UNITS OF FRAME)

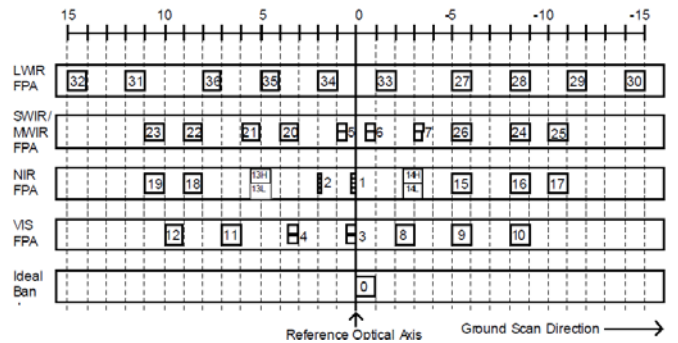| Band	Frame	Band	Frame	Band	Frame	Band	Frame
1	0.25	2	2	3	0.5	4	3.5
5	1	6	-0.5	7	-3	8	-2
9	-5	10	-8	11	7	12	10
13	5.5	14	-2.5	15	-5	16	-8
17	-10	18	9	19	11	20	-5
21	6	22	9	23	11	24	-8
25	-10	26	-5	27	-5	28	-8
29	-11	30	-14	31	12	32	15
33	-1	34	2	35	5	36	8

Fig. 3. The layout of MODIS FPA configuration. The four FPAs are vertically aligned in reference to the optical axis for direct comparison. The scale on the top is in units of frame.

frame ranges by different bands if their band locations on the FPAs are different. Table I lists the nominal values of the band locations relative to the MODIS B0, a virtual band located at the center of the FPA or its optical axis. If B0 captures the image of a target at time t_0, band i captures the same target at

$$t' = t_0 + \tau F_i, \tag{1}$$

where

τ : 333.333 μs

F_i: Location of band i's trailing edge relative to optical axis

The misregistration between the images of two bands i and j of the same target, in unit of frames, is then

$$\Delta F = F_i - F_j. \tag{2}$$

For example, the band position of B30 is -14, indicating that B30 views a certain target 14 clock periods earlier than B0. The B30 image of a target is captured 14 frames earlier than the B0 image of the same target, if there is no post-processing.

For convenience of downstream data processing, it is desired that the images of the same EV target of various bands are spatially co-registered in the along-scan direction, represented at the same frame number. To compensate the frame misregistration in (2), the image frames of different bands are co-registered by an on-board formatter. The captured images (called unformatted frames) of leading bands are firstly stored in a buffer of 30-frame deep in the formatter, waiting for the images of trailing bands to be collected.

Appropriate band-dependent time delay that is proportional to the band location is applied in the buffer: the delay for band i is $-\tau F_i$. The effect is, if band i captures a target Δt earlier than band j, the frame will be delayed Δt relative to band j in the buffer, until the image of the same target of band j being popped into the buffer. The maximum distance among the bands on the FPAs is 29 frames between B30 and B32. Therefore, within a period of time of 30τ, images from all bands containing the same ground target should be pumped into the buffer and co-registered. They are popped out of the formatter as a "formatted frame" and sent to ground for further processing [4]. For MODIS, the on-board co-registration is applied to EV data sectors, as well as SD, BB and SV data sectors. The residual misalignment among bands after the co-registration is the so-called band-to-band misregistration (BBR). The BBR of MODIS is monitored by the SRCA as well as other approaches [5, 6]. It has been stable during the mission lifetime, well within the specification of ±0.1 1 km pixels for most of the bands. This sub frame-level BBR is universal for all targets including EV scenes and is not the misregistration analyzed in this paper.

III. BAND MISREGISTRATION OF OBC IMAGES

While numerous MODIS products have proved that the on-board co-registration performs its designed functionality well for the "far-field" targets such as EV scene and the Moon, it has been noticed since pre-launch calibration test that a certain amount of band misregistration does exist for OBC images and has been considered during sensor design phase to determine how many good frames of each band are needed to view the OBC. The on-orbit observation of the misregistration is not straightforward because only the center portion of the OBCs are viewed during regular calibration, where the surface properties of the OBCs are mostly uniform. However, under certain circumstances, data sector rotation (SR) is implemented to the instrument. During the SR, the starting location of the EV data sector is delayed by pre-determined encoder counts so that the EV sector can continuously collect data when the detectors actually view the cavity rather than the nadir aperture door. Because the EV sector is 1354 frames wide, a large portion of the cavity including the OBCs can be continuously sampled.

There are multiple programmed settings of SR encoder numbers for MODIS. One setting was implemented during the series of satellite yaw maneuvers performed for Terra in 2002 and 2003 and for Aqua in 2002. The SD, SRCA, BB and SV can be completely imaged. Another setting is implemented at the time of roll maneuver scheduled for lunar calibration on a nearly monthly basis. SRCA BB and SV are completely imaged. The design of SR provides a unique opportunity to observe the complete OBCs including their boundaries and thus is critical to study the misregistration of OBC images.

A. Misregistration of SD Images

Figure 4 shows the spatial profile of Aqua MODIS SD, in unit of digital number (DN), in the along-scan direction based on the SD images acquired during a yaw maneuver with SR
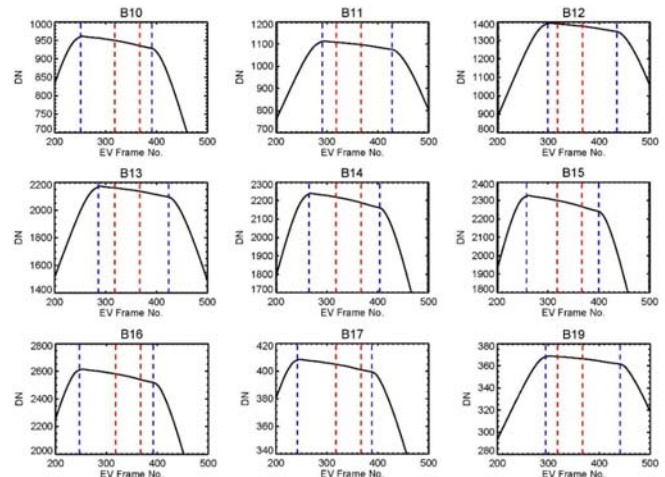

Fig. 4. The along-scan SD profiles for a few Aqua RSBs during a yaw maneuver with SDS closed. The two red dashed lines bracket the frame range used for SD calibration. The two blue dashed lines indicate the edges of the SD profiles calculated from the images.
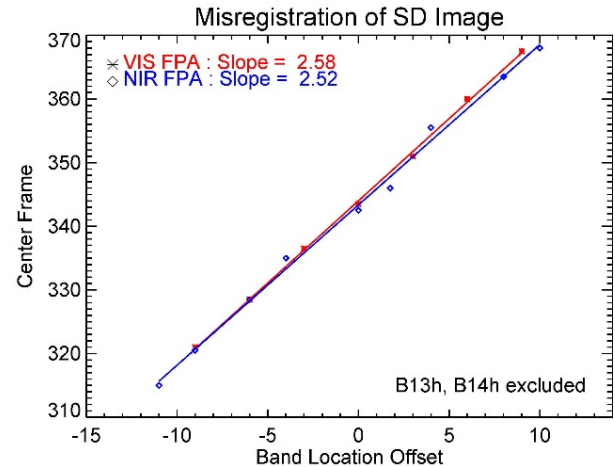

Fig. 5. The amount of band misregistration of SD images as a function of band location on the FPA for Aqua MODIS.

applied. The profile is calculated by taking the average of DNs over multiple scans with SD fully illuminated at the same solar angle range at which regular SD calibration is performed. The two red dashed lines bracket frame 318-367 of EV data sector, corresponding to the 50 frames of SD data sector during regular SD calibration. The frame range is determined by the counts of encoder delay SR setting and is thus a fixed number for all bands. The two blue dashed lines indicate the positions where the detector footprint starts to fall off the SD, which are calculated from the images themselves by evaluating the first derivative of the DN profile. Because the footprints of these bands are of similar sizes, the positions of the blue lines are indicators of the SD boundaries. It can be observed that the positions of the blue lines are band dependent. It indicates that the SD images of these bands are mis-registered in the along-scan direction. The observations made using the data of other yaw maneuvers show the same misregistration. The analysis is repeated for Terra MODIS with the same amount of misregistration observed as well.

It is noticed that the amount of the misregistration is directly related to the band location on the FPA. For the bands
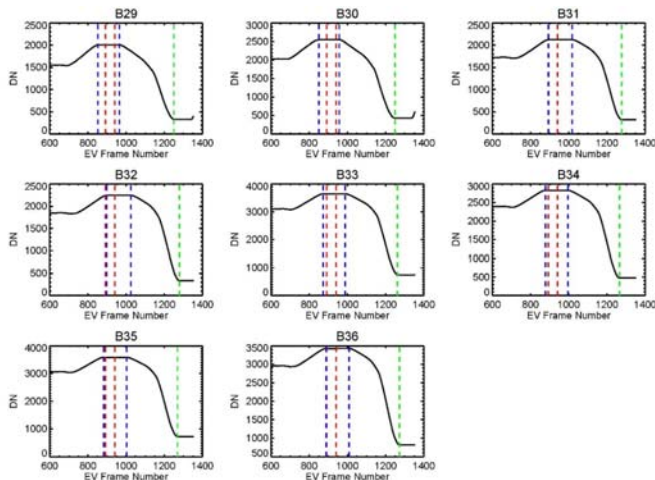
Fig. 6. The along-scan BB profiles for a few Aqua TEBs during a yaw maneuver with SDS closed. The two red dashed lines bracket the frame range used for BB calibration. The two blue dashed lines indicate the edges of the BB profiles calculated from the images. The green dashed line indicates the edge of the SV profile calculated from the images.

plotted in Fig. 4, B10 and B12 are located at the two ends of the VIS FPA and the misregistration between them is maximal. Also, B10 on the VIS FPA and B16 on the NIR FPA share the same band location, and there is no noticeable misregistration between them. To further analyze the relationships between the amount of misregistration and the band location, the centers of the SD images are calculated for each band by averaging the positions of the two blue dashed lines and plotted as a function of the band location, as is shown in Fig. 5. They are almost proportional to each other and the slope C_0 is calculated through linear regression. C_0 from various sets of yaw maneuver data are consistent, ranging from 2.51-2.59. Data of some bands cannot be used in the calculation: the SD images of ocean color bands B8-B16 are saturated with SD screen open and the saturation distorts the shapes of the SD images. B13h and B14h are excluded from the calculation because their SD images are saturated even when the SD screen is closed.

At the two extremes B17 and B19, the maximum of the misregistration is about 55 frames, larger than the width of the SD sector. Even considering the sizable detector footprint on the SD, the results disclose the fact that these two bands are calibrated by considerably different portions of the SD. Therefore, the non-uniformity of the SD surface properties, if there is any, will introduce extra band dependence to the calibration on top of widely known band dependency due to wavelength difference.

B. Misregistration of BB and SV Port Images

Figure 6 shows the images of the BB and SV port together acquired during one Aqua yaw maneuver. Again, the two red dashed lines bracket 50 frames corresponding to the BB data sector at regular operation, which are band independent. The two blue dashed lines indicate the positions where the detector footprint starts to fall off the BB. Band-to-band misregistration are again observed among the BB images. The maximal misregistration occurs between B30 and B32, which are located at the two ends of the LWIR FPA (Fig. 3). The green
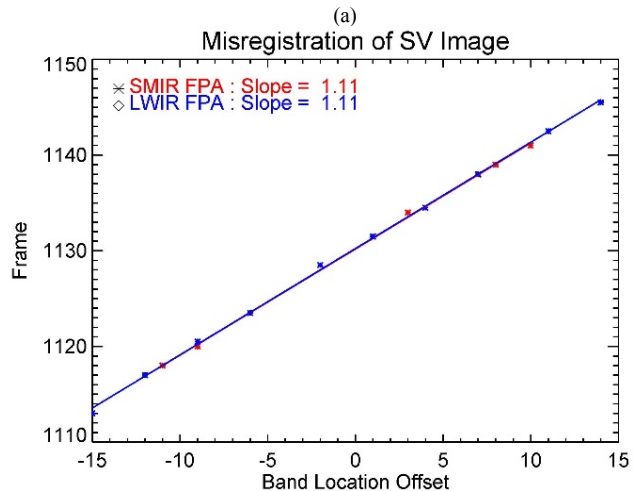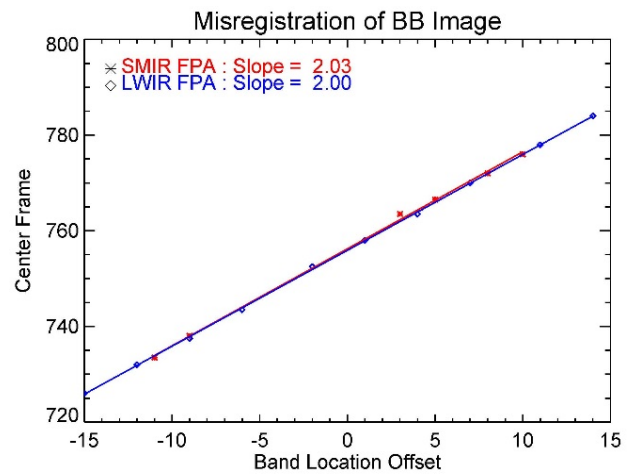

Fig. 7. The amount of band misregistration of (a) BB images and (b) SV edge images as a function of band locations on the FPA for Aqua MODIS.

dashed line on the right side of the plot indicates the position of the top (left in the plot) boundary of the SV port. For the SR setting applied during yaw maneuver, the SV is observed at the end of the EV data sector. We can see the images of some bands contain the bottom (right in the plot) boundary of the SV port while the images of other bands do not contain it. It demonstrates that there is a band-to-band misregistration for the images of SV port as well. The same misregistration can be observed for other yaw maneuvers and for Terra MODIS as well.

Similar to the analysis of SD images, the centers of the BB images and SV boundaries are calculated for each band and plotted as a function of the band location, as is shown in Fig. 7. The slopes C_0 of the BB images are calculated for each observation, and range from 2.00-2.05, less than the slope derived from SD images. The slopes of the SV port boundary images range from 1.09-1.12. The fire detection band B21 is excluded from the calculation because its detector gain is set at a low level leading to very noisy BB image. For B31 and B32, it is noticed that their BB images captured through BB data sector are slightly off the uniform portion of the BB. This phenomenon has been observed during pre-launch testing and certainly negatively impact the calibration of these bands.
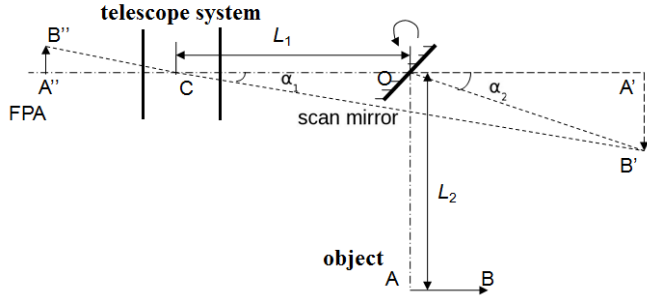
Fig. 8. The Simplified imaging geometry for the MODIS SD calibration with track direction vertical to the paper plane: the target AB is imaged to A'B' by the scan mirror and then imaged to A"B" by MODIS telescope system onto the FPA. OA = OA' = L_2, AB = A'B".

Overall, the band-to-band misregistration is observed for all OBCs, which are "near-field" targets comparing to the "far field" EV scenes and the Moon whose images are free of misregistration. The amount of the misregistration is linearly proportional to the band position at the FPA. The slope C_0 depends on the targets and decreases for SD, BB, SV port and "far field" targets, whose C_0 is zero for no misregistration. Throughout MODIS mission, the misregistration has also been regularly observed for BB and SV during lunar roll maneuver when SR at different encoder count delay is applied, which does not cover SD. The amount of misregistration has been stable.

C. Root Cause of the Misregistration

A sketch of the MODIS SD calibration imaging geometry is provided in Fig. 8. The two vertical bold lines that bracket point C represent the MODIS telescope, which is an afocal system with two reflector mirrors. Their positions are fixed in MODIS cavity. It is the rotation of a scan mirror centered at O that directs the light from various incident angles to the telescope. Assume A" and B" are the band locations of B0 and band i at the FPA, respectively and they are one frame or clock period apart. At time t_0, the nadir ground target A is imaged by the MODIS scan mirror to A' first and then by the MODIS telescope to A" (B0) at the FPA. At the same time, target B is imaged to B' and then B" (band i). The angular distance between the two targets is α_1 in reference to C, the principal point or nodal point of the primary mirror of the telescope, which is also shared by the secondary mirror.

Now, if the scan mirror rotates a time period of Δt, B will be imaged by the scan mirror to A' and then imaged to A" or B0. It means that B0 captures the image of B Δt later than band i. The time it takes depends on the angular distance α_2 between the two targets in reference to O, the scan mirror, given a constant rotating speed. When the targets are far away from the telescope (ground targets or Moon, for example), α_1 and α_2 are essentially equal. When the target approaches the scan mirror, however, the target's angular position to the scan mirror α_2 becomes larger than its angular position to the telescope α_1. Then it will take longer time than τ for the scan mirror to direct the light from B to A" (B0). The closer the target distance, the greater the difference between α_1 and α_2 and thus the delay time Δt is longer.

The actual delay time can be calculated from instrument parameters. If the target locates at the infinity, α_1 equals to α_2 and then Δt equals to τF_i. Because the scan mirror rotates at a constant speed, Δt is always proportional to α_2. Based on the geometry in Fig. 8, the delay time for a target at finite distance is then

$$\Delta t = \frac{\alpha_2}{\alpha_1} \tau F_i = \frac{arc\tan\left(\dfrac{h}{L_2}\right)}{\arctan\left(\dfrac{h}{L_1 + L_2}\right)} \tau F \approx \frac{L_1 + L_2}{L_2} \tau F_i , \tag{3}$$

where

L_1: the distance from the scan mirror to the focus of the 1st primary mirror;

L_2: the distance from the scan mirror to the target;

h: the distance of AB, which is also the distance of A'B' for a flat scan mirror.

As is introduced before, MODIS formatter always applies a delay time τF_i for band i to compensate to rotation of the scan mirror. The delay after the compensation, which is

$$\Delta F_i = \frac{\Delta t}{\tau} = \frac{t - t'}{\tau} \approx \frac{\dfrac{L_1 + L_2}{L_2} \tau F_i - \tau F_i}{\tau} = \frac{L_1}{L_2} F_i = C_0 F_i , \tag{4}$$

is then the misregistration in the along-scan direction observed above, Since L_1 is fixed for the optical system, the slope of the misregistration is then a function of L_2, which is the target distance to the scan mirror.

For MODIS, the nominal value of L_1 is 1330.43 mm. When the target is at far-field so that $L_2 \gg L_1$, the coefficient is essentially zero. Clearly it implies that there is no band-to-band misregistration for EV images or lunar images. When the target is at near-field when L_2 is comparable to L_1, the misregistration becomes noticeable. The distance of the SD to the scan mirror is 516.5 mm, which results in a linear coefficient of 2.58 for SD images. The number agrees well with the value calculated from the SD images directly presented earlier. The accurate positions of the BB and the SV port are unknown but they are reasonably close to the values needed to get the C_0 calculated from the BB and SV images.

IV. IMPACT TO CALIBRATION

The misregistration of the OBC images discussed in this paper has noticeable, although limited, impact to MODIS calibration: since different bands view different locations of the OBCs, the calibration references are actually band dependent if the surface properties of the OBCs are not spatially uniform. Band dependent calibration errors will be introduced if the band dependency is not considered. This effect need to be separated from the more obvious band dependency caused by wavelength difference. In this section, the impact of the misregistration to SD calibration and BB calibration is investigated.

A. Undesired Seasonal Oscillation in m_1 Trending

The MODIS high-gain ocean color bands B8-B16 are calibrated with a SD screen (SDS) to avoid detector saturation [7]. Consequently, the characterization of the vignetting (transmission) function (VF) of the SD screen is necessary for
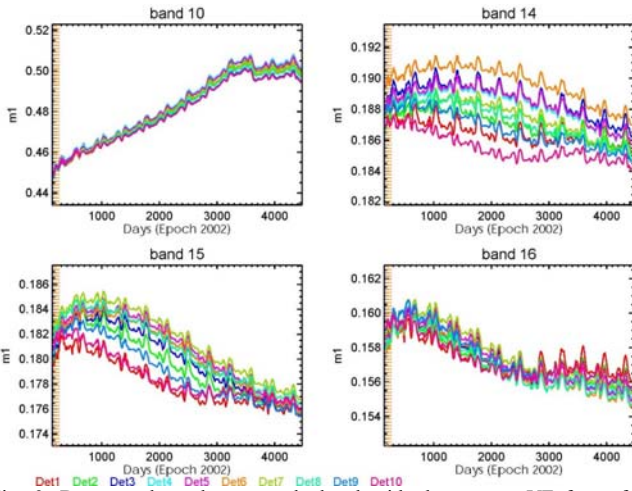
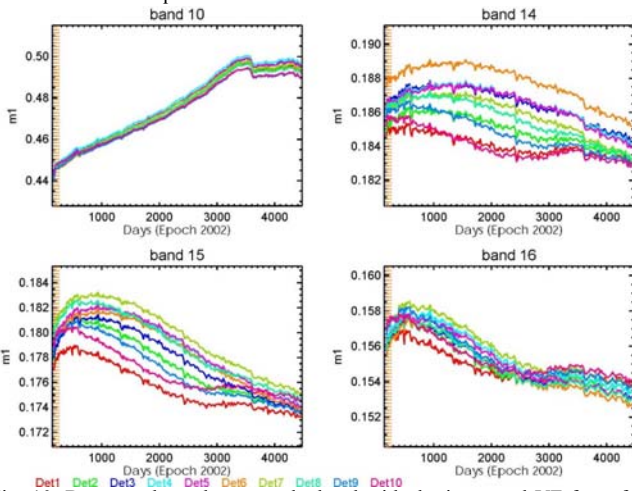Fig. 9. Detector dependent m_1 calculated with the current VF for a few selected bands of Aqua MODIS.

Fig. 10. Detector dependent m_1 calculated with the improved VF for a few selected bands of Aqua MODIS.
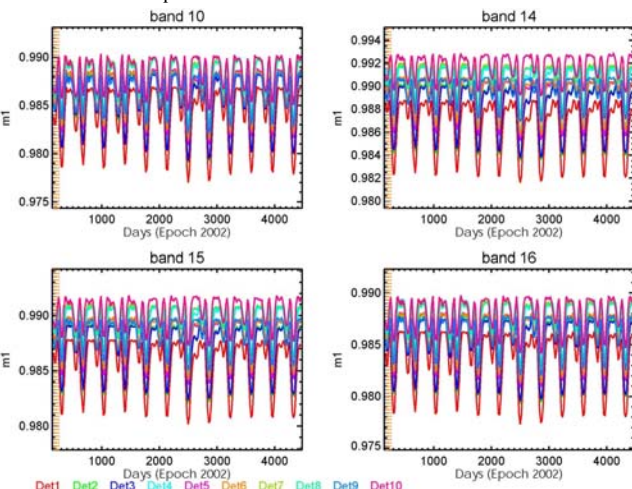

Fig. 11. The ratios of the detector dependent m_1 derived with the improved VF and current VF for a few selected bands of Aqua MODIS.

calibrating the detector gain coefficient m_1 of these bands, which is calculated by the equation

$$m_1 = \frac{BRF(\theta_{SD}, \varphi_{SD}) \cos \theta_{SD}}{dn^*_{SD,closed} \cdot d^2_{Earth-Sun}} \cdot \Delta_{SD} \cdot \Gamma(\theta_{SD}, \varphi_{SD}) \qquad (5)$$

Here BRF is the SD bi-directional reflectance factor. θ_{SD} is the solar zenith angle and ϕ_{SD} is the solar azimuth angle. $d_{Earth-Sun}$ is the Earth-Sun distance. $dn^*_{SD,closed}$ is the detector
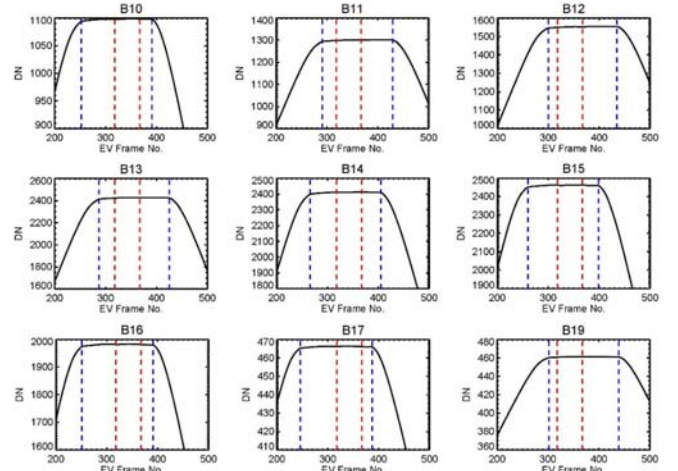

Fig. 12. The along-scan SD profiles for a few Terra RSBs during a yaw maneuver with SDS closed. The two red dashed lines bracket the frame range used for SD calibration. The two blue dashed lines indicate the edges of the SD profiles calculated from the images.

response in digital number, readout from the SD sector, after the correction of instrument background signal and instrument temperature effect. The subscript "closed" indicates that the data are acquired with the SDS closed. Γ is the SDS VF, which is also a function of solar angles. When the SDS is in its open position, the m_1 is calculated similarly, except that the VF term is dropped and $dn^*_{SD,closed}$ can be replaced by $dn^*_{SD,open}$.

Since there was no pre-launch characterization of VF for MODIS, a series of yaw maneuvers were carried out on-orbit for both Terra and Aqua to enable its on-orbit characterization. The VF currently used in m_1 calculation was derived from the yaw data of the low-gain bands B1-B7 and B17-B19, and applied to the high-gain ocean color bands [8]. The approach is based on the assumption that the VF should be band independent since the sunlight attenuation by the SDS is wavelength independent and all bands scan across the SD at the same positions according to MODIS design.

Seasonal oscillation of up to 1% has been observed in the long-term trending of the m_1 of the ocean color bands calibrated with the SDS closed, as is shown in Fig. 9 for a few bands of Aqua MODIS. Each trending curve represents the m_1 of a detector. The seasonal oscillation is an indication of error in one of the terms in the calibration equation (5). The reason is that most of them, as well as their systematic error if there is any, are functions of the solar azimuth angle ϕ_{SD} that oscillates on a yearly basis for MODIS. When the seasonally oscillated error is carried over into m_1, which is supposed to change smoothly on-orbit, via (5), seasonal oscillation in m_1 trending is introduced. The seasonal oscillation of the non-ocean color bands calibrated without the SDS, however, show much less oscillation, which indicates that the error in VF characterization is the major source to the oscillation of m_1.

B. Improved Band-Dependent SDS VF

The SDS is a metal plate with a uniformly distributed pinhole array on it [9]. The SDS VF is determined by the size and density of the pinholes images on the SD within the
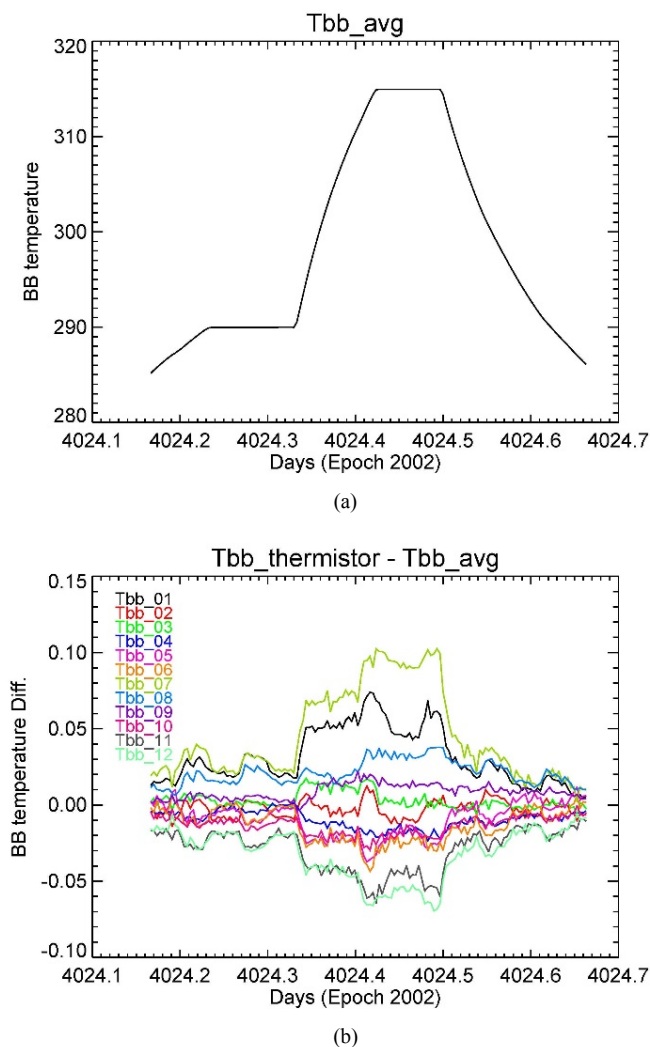
(a)

(b)

Fig. 13. The (a) band-averaged and (b) detector-difference temperatures of the BB during an Aqua BB WUCD calibration event.

footprint of the MODIS detector. The screen is not parallel to the SD plane, thus the images of the pinholes on the SD are not uniformly distributed. It means that the VF is a localized function on the SD, depending on the position of the detector footprint on the SD. Within a scan, the footprint moves across the SD in the along-scan direction and VF changes from frame to frame. Within a band, its detectors are assembled in the along-track direction, so their footprints on the SD offset from each other in that direction. This introduces the detector dependency of the VF. SD calibration uses the observation of the SD in 50-frame wide SD data sector. Because of the band-to-band misregistration for the SD discussed in this paper, the 50 frames of SD images of two bands correspond to different spots on the SD when the locations of the bands are different on the FPA. The VFs of the two bands are thus different. Therefore, the VF is band dependent. There are other effects that potentially introduce band dependency, such as the Earthshine effect [10]. However, these impacts are much less significant than band-to-band misregistration and have strong spectral dependency that is inconsistent with the oscillation patterns observed in m_1 trending.

With better understanding of the band and detector

dependency of the VF and the determination of the amount of band misregistration for the SD, a set of improved band-and-detector dependent VF has been developed for Aqua MODIS and tested [11, 12]. The m_1 of the ocean color bands calibrated with the improved VF is shown in Fig. 10 for the exampled bands. The impact of the VF improvement to the m_1 calculation, which is the ratio of the m_1 in Fig. 10 and Fig. 9, is shown in Fig. 11 for these bands. The improvement is less significant for other bands. The improvement of m_1 calculation helps to reduce the seasonal oscillation observed in the long term trending of current m_1. Other than the reduction of oscillation, the VF also introduces a detector dependent offset between the absolute values of current m_1 and new m_1. This is predictable because the calculation of current m_1 uses the same VF for all detectors and the new m_1 uses a detector-dependent VF.

Other bands show similar improvements although the significance of the improvement is band-dependent. It is noted that the amount of band misregistration is a function of band location, not the center wavelength of the band. Then the improvement of the m_1 calculation is not associated with the center wavelength of a band but its location of the band at the FPA. The biggest improvement is observed in B9-B10 and B13-B16, which have longer wavelengths and their calibrations have been considered to be more reliable than the shorter wavelength bands.

The same methodology is applied to Terra MODIS and its m_1 calculation is similarly improved. However, comparing the along-scan profile of Terra MODIS SD during a yaw maneuver with SDS closed, which is plotted in Fig. 12, with that of Aqua MODIS in Fig. 4, the SDS VF of Terra MODIS is spatially more uniform across the SD for unknown reason. Therefore, the impact of band misregistration is less significant and the improvement of m_1 calculation when considering the effect is less for Terra MODIS.

B. Non-uniformity of BB

The temperature of the BB is monitored by 12 thermistors at various locations. While the BB has been proven to be spatially uniform in general, a small temperature gradient does exist across the BB [13]. BB warm-up-cool-down (WUCD) activity is scheduled for MODIS on a quarterly basis to calibrate the gain coefficients of TEB detectors. During the BB WUCD, the blackbody is heated from its operational temperature of 290 K up to 315 K for Terra and 285 K to 315 K for Aqua, and then cooled to ambient temperature of approximately 270 K. The temperatures measured by the BB thermistors during a typical Aqua WUCD calibration event are shown in Fig. 13. Ideally, since different bands observe different locations on the BB and since there exists a temperature gradient, a set of band dependent weight needs to be applied to the thermistors to determine the BB temperatures corresponding to each band. However, the maximum gradient is less than 0.05 K at regular operation and 0.15 K at the peak temperature of the WUCD. Most of the effects are also smoothed out when 50 frames of BB images are averaged. As a result, the impact of the OBC misregistration to the TEB

calibration is minimal.

V. CONCLUSION

This paper investigates the band-to-band misregistration phenomenon observed in the OBC images of MODIS. It shows that the misregistration is significant at up to 60 frames. The amount of the registration is proportional to the band location at the FPA, and is inversely proportional to the distance between the target and scan mirror. The cause of the misregistration is identified as a fact of instrument design that the scan mirror is displaced from with the common focal (nodal) point of the telescope system.

The impact of the misregistration to MODIS SD and BB calibration is analyzed in this study. The characterization of the SD screen VF has been improved for MODIS, as well as the m_1 calculation. It is shown that the misregistration contributes to the majority of the band dependency of the VF. The seasonal oscillation in the the m_1 trending is significantly reduced. In general, while the misregistration should be considered in the design of future sensors with similar scanning mechanism, its impact can be minimal if the OBCs are spatially uniform and wide enough to cover the footprints of all bands during calibration.

This study also demonstrates that occasional observations of the cavity through SR, or simply expanding the OBC data sectors can provide useful data to better understand the calibration process.

REFERENCES

[1] W. L. Barnes, T. S. Pagano, and V. V. Salomonson, "Pre-launch characteristics of the Moderate Resolution Imaging Spectroradiometer (MODIS) on EOS AM-1," *IEEE Trans. Geosci. Remote Sens.* vol. 36, no. 4, pp. 1088-1100, 1998.
[2] W. L. Barnes, X. Xiong, and V. V. Salomonson, "Status of Terra MODIS and Aqua MODIS," *J. Adv. Space Res.* vol. 32, no. 11, pp. 2099-2106, 2003.
[3] Raytheon Company, "MODIS command, telemetry, science and engineering description," 2000.
[4] MODIS science data support team, "MODIS level 1A earth location: algorithm theoretical based document version 3.0," document No.: SDST-092, 1997.
[5] X. Xiong, N. Che, and W. L. Barnes, "Terra MODIS on-orbit spatial characterization and performance," *IEEE Tran. Geosci. Remote Sens.* vol. 43, no. 2, pp. 355-365, 2005.
[6] X. Xiong, J. Sun, and W. L. Barnes, "Using the Moon for MODIS on-orbit spatial characterization," *Proc. SPIE*, vol. 5234, pp. 480-487, 2003.
[7] X. Xiong, K. Chiang, J. Esposito, B. Guenther, and W. L. Barnes, "MODIS on-orbit calibration and characterization," *Metrologia*, vol. 40, pp. 89-92, 2003.
[8] X. Xie, X. Xiong, D. Moyer, J. Sun, X. Liu, and W. L. Barnes, "Analysis of MODIS solar diffuser screen vignetting function," *Proc. SPIE*, vol. 5882, pp. 271-281, 2005.
[9] E. Waluschka, "MODIS solar diffuser - modeled and actual performance," *Proc. SPIE*, vol. 4483, pp. 146-155, 2002.
[10] R. Wolfe, W. Esaias, A. Lyapustin, and X. Xiong, "MODIS solar diffuser Earthshine modeling and analysis," *Proc. SPIE*, vol. 6296, pp. 629606, 2006.
[11] Z. Wang, X. Xiong, "Characterization of MODIS SD screen vignetting function using observations from spacecraft yaw maneuvers," *Proc. SPIE*, vol. 7452, pp. 745217, 2009.
[12] Z. Wang, X. Xiong, and W. L. Barnes, "Further Investigation on MODIS Solar Diffuser Screen Vignetting Function and Its Implementation in RSB Calibration," *Proc. SPIE*, vol. 8153, pp. 815307, 2011.
[13] X. Xiong, S. Madhavan, "Characterization of Terra MODIS blackbody uniformity and stability," *Proc. SPIE*, vol. 7807, pp. 78081E, 2010.

Zhipeng (Ben) Wang (M'16) received a B.S. and M.S. degrees in Optoelectronics from Department of Precision Instrument and Mechanology, Tsinghua University, Beijing, China, in 2000 and 2003, respectively, and a Ph.D. degree in optics from the University of Arizona, Tucson in 2008.

He is currently a Lead Research Scientist at Science Systems and Applications Inc., Greenbelt, MD, working with the NASA MODIS Characterization Support Team (MCST) and VIIRS Characterization Support Team (VCST).

Xiaoxiong (Jack) Xiong is an optical physicist at NASA Goddard Space Flight Center (GSFC). He is currently serving as the MODIS Project Scientist and the technical lead for both the MODIS Characterization Support Team (MCST) and the VIIRS Characterization Support Team (VCST).

He received a B.S. degree in optical engineering from Beijing Institute of Technology, Beijing, China and a Ph.D in physics from University of Maryland, College Park, Maryland. Before joining the NASA/GSFC, Dr. Xiong had also worked in the fields of optical instrumentation, nonlinear optics, laser and atomic spectroscopy, and resonance ionization mass spectrometry at universities, industry, and at the National Institute of Standards and Technology (NIST).